Materials Research Proceedings **26** (2023) 455-460 https://doi.org/10.21741/9781644902431-74

The minimum variance distortionless response beamformer for damage identification using modal curvatures

Annamaria Pau[1, a *] and Ugurcan Eroglu[2,b]

[1]Department of Structural and Geotechnical Engineering, Sapienza University of Rome, Italy

[2]Department of Mechanical Engineering, MEF University, Istanbul, Turkey

[a]annamaria.pau@uniroma1.it, [b]erogluug@mef.edu.tr

* corresponding author

Keywords: Damage Identification, Modal Curvatures, Inverse Problems

Abstract. This study presents a damage identification procedure in beams based on the use of beamforming algorithms, which are mostly utilized in inverse problems of source identification and image reconstruction. We choose the modal curvatures as observed quantities and compare the performance of the Bartlett beamformer, minimum variance distortionless response (MVDR) processor, and of a conventional objective function based on the modal curvatures. By means of a set of experiments, we show that the MVDR processor can overcome some of the difficulties encountered with other estimators, especially in cases of slight damage, or damage located between two sensors.

Introduction

Numerous studies have proven that the use of modal quantities is a very effective strategy to locate damage [1]. Among different modal quantities, modal curvatures stand out for their low sensitivity to environmental and operational conditions, and better performance in case of slight damage [2,3]. When solving the related inverse problem, it is important to apply a robust estimator (or processor), which may improve the quality of the solution, especially in the presence of disturbance due to operating conditions, noisy data, and modelling errors.

The Minimum Variance Distortionless Response (MVDR) data processor [4], also named beamformer, is an estimator successfully applied in image-reconstruction techniques based on the wave response, for instance, to locate sources in oceans, but also to reconstruct the image of defects in plates and solids [5]. It is based on the comparison of modelled responses (replica vector) to data received by an array of sensors. Compared to other beamformers, the MVDR has proved its effectiveness in minimizing noise, thus providing images of very good quality. The use of the MVDR processor can be viewed as an approach to the solution of an inverse problem, with potential applications to a broader range of problems in which the forward solutions are computable and measurable, especially regarding the field of structural vibrations, where the use of such estimator has not received attention in the literature to date. We aim at applying the MVDR beamformer to damage identification in beams, using modal curvatures as measured response quantities. To this aim, we assess the performance of the MVDR processor in identifying damage in pseudo-experimental and experimental cases with different location and intensity. Comparisons of the MVDR estimates to those of the Bartlett beamformer, and of a conventional objective function based on the modal curvatures are carried out. For the sake of brevity, this paper only reports some experimental results, while the full analysis is presented in [7].

Numerical Model

The direct problem is solved by means of a 2D finite element (FE) plane stress analysis. This model is used to obtain natural frequencies and mode shapes of a free-free beam of length L, with

Materials Research Proceedings **26** (2023) 455-460 https://doi.org/10.21741/9781644902431-74

a notch of small extension b^{D}, located at position S^{D}, measured from left end of the beam (see Fig.1). The cross-section of the beam is rectangular with height H^{U} and width b. The notch is modelled as a height reduction to the value H^{D} in a stretch b^{D}. We define damage by two non-dimensional variables, namely, its location $s^{\mathrm{D}}=S^{\mathrm{D}}/L$, and the residual height of the cross-section, $h^{\mathrm{D}}=H^{\mathrm{D}}/H^{\mathrm{U}}$, collected in the vector, $\overline{\boldsymbol{x}} = \{s^D, h^D\}^T$.

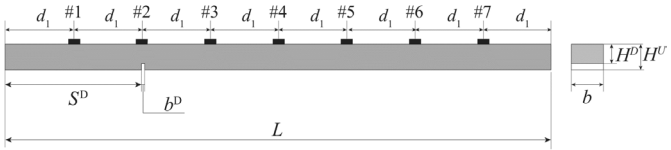

L=520 mm H^U=15 mm b=30 mm d_1=65 mm b^D=1 mm
E= 2.13*10^{11} N/m^2 ρ=7860 kg/m^3

Figure 1. *Schematic representation of the beam used in benchmark case*

The numerical model is used for the construction of the replica vectors via sweeping the damage location from $s^D_{min} = 0.04$ to $s^D_{max} = 0.96$ in 48 steps, and the residual height from $h^D_{min} = 0.06$ to $h^D_{max} = 0.97$ in 30 steps. For all the analyses we evaluate the longitudinal modal strains ε at m=7 equally spaced points, as numbered in Fig.1, and derive modal curvatures using the kinematic relation $\chi=\varepsilon/H^U/2$ of the Euler-Bernoulli beam theory.

Experimental Study

The experimental setup is illustrated in Figure 2. The beam was excited by an instrumented hammer, at points #8 or #9, and the response was measured using seven strain gauges and two accelerometers. The tests were repeated ten times per each point of application of the forcing function. The applied impulsive force is capable of exciting frequencies up to 3000 Hz, which enables determining the first three natural frequencies. Accelerometers at points #8 and #9 are used for modal curvature normalization [6].

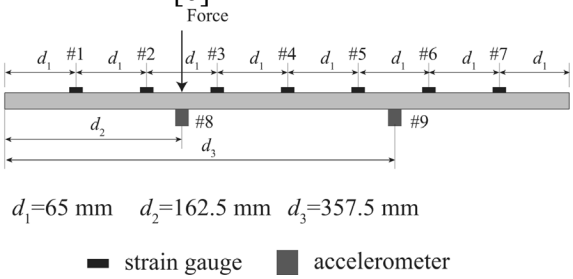

Figure 2. *Schematic of the experimental setup*

We consider two cases which we label Case A, and Case B. In the former, damage is located at s^{D} = 0.25, that is, under sensor #2, while in the latter damage is between sensors #3 and #4, with s^{D} = 0.4375. In both cases we consider two damage severities which correspond to nominal residual heights h^{D} = 0.75 (D1) and h^{D} = 0.5 (D2). In all cases the damage extension is fixed, with b^{D} = 1 mm.

The numerical and experimental curvatures of the first three modes for Case A and Case B are presented in Fig.3. Overall, a very good agreement is observed in both cases regarding the form of the curves. In Case A, the localized effect of damage can be captured by the sensor #2 and the curvature exhibits a distinct change, providing a strong hint at the location of damage. In Case B, instead, the localized effect cannot be captured, which makes locating the damage more difficult.

Materials Research Proceedings **26** (2023) 455-460 https://doi.org/10.21741/9781644902431-74

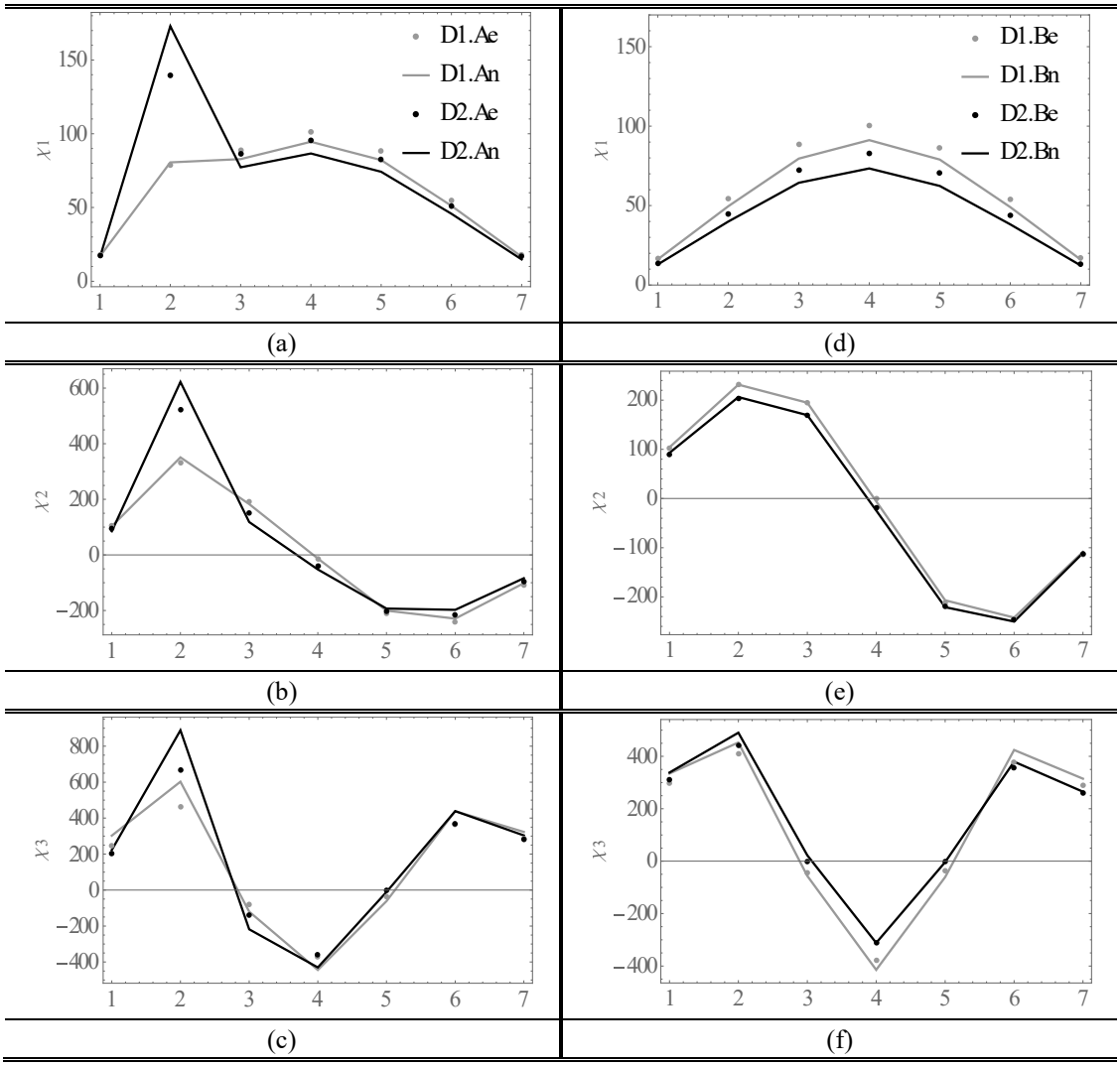

Figure 3. *Numerical and experimental modal curvatures for Cases A (a-c) and B (d-f).*

Inverse Problem via MFP Algorithms

The direct solution of the free-vibration problem provides the replica vectors $\boldsymbol{\chi}_i(\overline{\boldsymbol{x}}) \in \mathbb{R}^m$, which list the mass-normalized modal curvatures of the i^{th} mode at m sensor points. The beamformers evaluate the correlation between the normalized replica vector,

$$\overline{\boldsymbol{\chi}}_i(\overline{\boldsymbol{x}}) = \boldsymbol{\chi}_i(\overline{\boldsymbol{x}})/\|\boldsymbol{\chi}_i(\overline{\boldsymbol{x}})\|, \tag{1}$$

and the data vector which lists mass-normalized modal curvatures obtained by experimental or pseudo-experimental measurements, $\boldsymbol{d}_i(\overline{\boldsymbol{x}}) \in \mathbb{R}^m$, for the i^{th} mode. Finding the damage parameter set which provides the best correlation with the measured data requires collecting the values of response data in the parameter space $[s^D_{min}, s^D_{max}] \times [h^D_{min}, h^D_{max}]$, which is performed by the 2D FE procedure described beforehand.

Bartlett Beamformer The Bartlett beamformer is a basic processor which has been used almost in all the studies about matched field processors (MFP) for comparative purposes. Simply, it is the average of the projection of the data vector onto the replica vector, and it can be written in terms of the cross-spectral density matrix (CSDM) of data, $\boldsymbol{K}_i = \boldsymbol{d}_i \boldsymbol{d}_i^T$. The expression for the Bartlett Beamformer for individual modes and their superposition are given below.

$$B_{Bart,i}(\overline{\boldsymbol{x}}) = \overline{\boldsymbol{\chi}}_i^T(\overline{\boldsymbol{x}}) \boldsymbol{K}_i \overline{\boldsymbol{\chi}}_i\ (\overline{\boldsymbol{x}}), \quad B_{Bartlett}(\overline{\boldsymbol{x}}) = \sum_{i=1}^{3} B_{Bart,i}(\overline{\boldsymbol{x}}). \tag{2}$$

Materials Research Proceedings **26** (2023) 455-460 https://doi.org/10.21741/9781644902431-74

This processor has many side lobes even in case of perfect pseudo-experimental data. This drawback is overcome by the adaptive filtering of data, which leads to different processors, one of which is the MVDR beamformer.

Minimum Variance Distortionless Response (MVDR) Beamformer Trying to minimize the projection except for the best match, we have [4]:

$$B_{MVDR,i}(\overline{\boldsymbol{x}}) = \left[\overline{\boldsymbol{\chi}}_i^T(\overline{\boldsymbol{x}})\boldsymbol{K}_i^{-1}\overline{\boldsymbol{\chi}}_i\ (\overline{\boldsymbol{x}})\right]^{-1}, \quad B_{MVDR}(\overline{\boldsymbol{x}}) = \sum_{i=1}^{3} B_{MVDR,i}(\overline{\boldsymbol{x}}). \tag{3}$$

Here we note that the CSDM is usually ill-conditioned which makes its inversion not a straight-forward task. We improve its conditioning using a diagonal loading technique, with a magnitude of $10^{-6}\mathrm{tr}\boldsymbol{K}_i$.

Objective Function A widely used objective function which measures the difference between replica vector and the measurement is:

$$H(\overline{\boldsymbol{x}}) = \sum_{i=1}^{3} \left\| \overline{\boldsymbol{\chi}}_i(\overline{\boldsymbol{x}}) - \overline{\boldsymbol{d}}_i(\overline{\boldsymbol{x}}) \right\|, \quad \overline{\boldsymbol{d}}_i(\overline{\boldsymbol{x}}) = \frac{\boldsymbol{d}_i(\overline{\boldsymbol{x}})}{\|\boldsymbol{d}_i(\overline{\boldsymbol{x}})\|}. \tag{4}$$

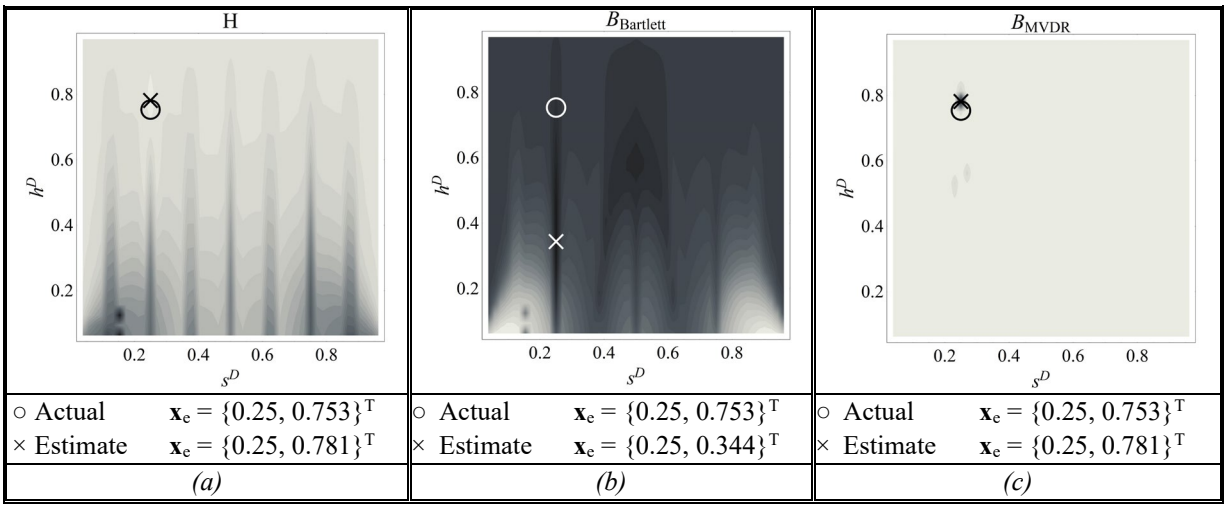

○ Actual	$\mathbf{x}_e = \{0.25, 0.753\}^T$	○ Actual	$\mathbf{x}_e = \{0.25, 0.753\}^T$	○ Actual	$\mathbf{x}_e = \{0.25, 0.753\}^T$
× Estimate	$\mathbf{x}_e = \{0.25, 0.781\}^T$	× Estimate	$\mathbf{x}_e = \{0.25, 0.344\}^T$	× Estimate	$\mathbf{x}_e = \{0.25, 0.781\}^T$
(a)		*(b)*		*(c)*	

Figure 4. *Contour plots and estimates of the objective function a), Bartlett beamformer b) and MVDR c) for D1.A.*

Fig.4 shows the contour plots of the different estimators and reports the related estimates of the damage parameters. Note also that the reported values of h^D slightly differ from the nominal ones for they were updated with their experimental measurement with a caliber. The correct value is denoted by a circle and the estimate by a cross. Overall, we see that the objective function and MVDR are very accurate in determining both location and severity of damage, while the Bartlett beamformer overestimates the severity but captures the correct location. Objective function and Bartlett beamformer admit many local extrema and side lobes, while MVDR remarkably surpasses them especially in terms of damage intensity resolution.

The estimates in the case of a more severe damage are reported in Fig. 5. We see a pattern very similar to the previous case in which the estimates of the objective function and MVDR are accurate, but the Bartlett beamformer overestimates damage severity.

In case of damage in between sensors #3 and #4, the identification is more difficult since the local effects of damage cannot be captured by one of the sensors (Fig. 3). This is reflected in Fig. 6; the objective function has wider flat valleys, many local maxima are apparent in Bartlett beamformer, and MVDR has many side lobes even though their order is smaller than the global

Materials Research Proceedings **26** (2023) 455-460 https://doi.org/10.21741/9781644902431-74

maxima. When damage is more severe (Fig. 7), the estimate of Bartlett beamformer is improved, however, it is still less accurate than those of the objective function and MVDR.

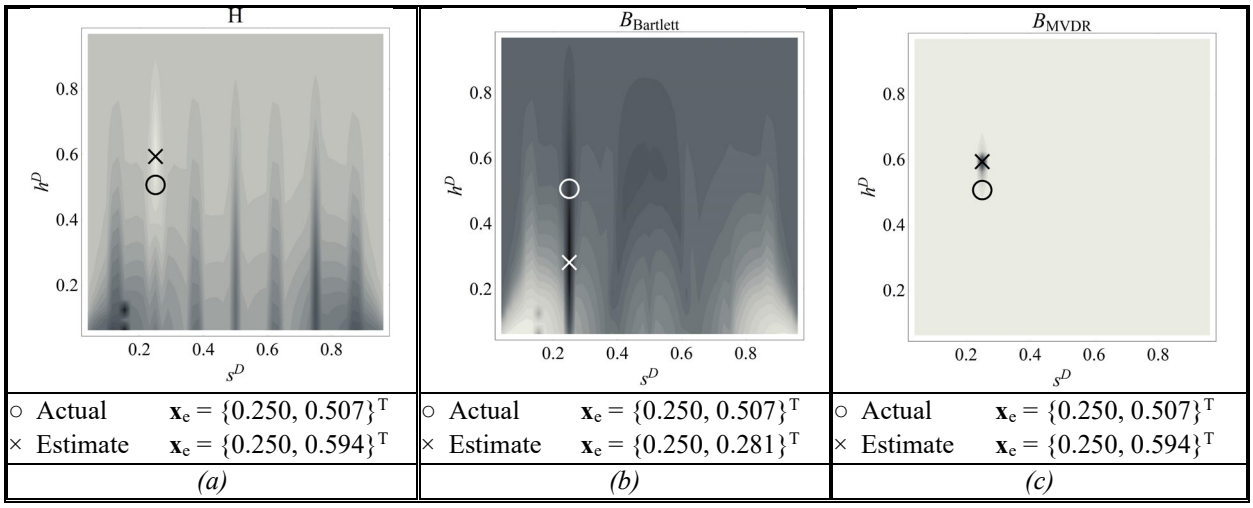

Figure 5. *Contour plots and estimates of the objective function a), Bartlett beamformer b) and MVDR c) for D2.A.*

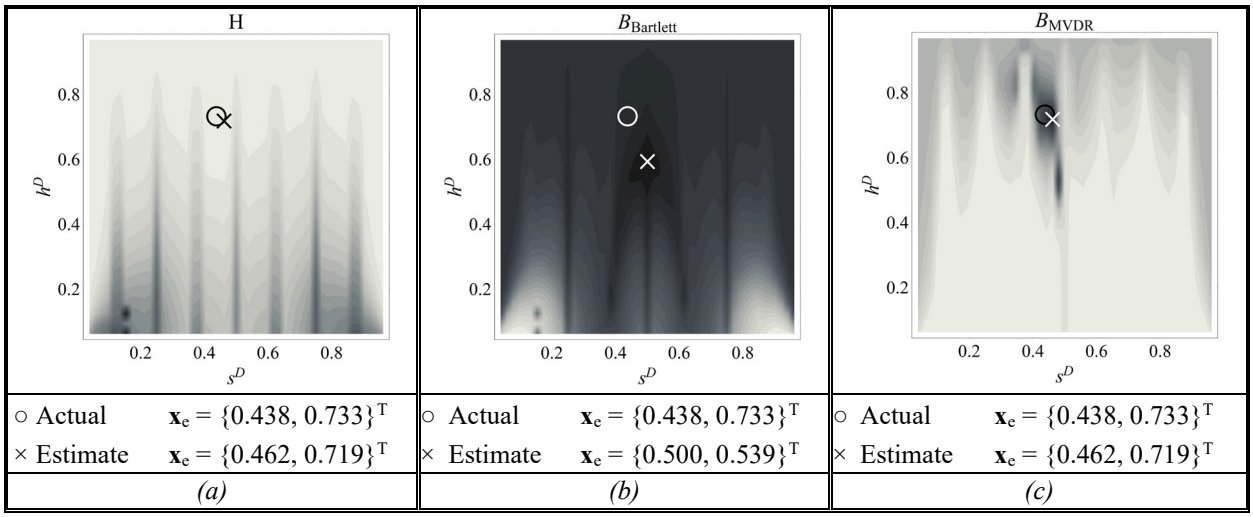

Figure 6. *Contour plot and estimates of the objective function a), Bartlett beamformer b) and MVDR c) for D1.B.*

The overall estimates of different techniques for all the cases we considered here are summarized in Table 1. We see that the minimization of a suitable objective function and the MVDR provides identical results in these cases; however, the extrema of the latter are always more distinct than the former, which is a strong hint on higher reliability of MVDR.

Table 1. *Absolute errors of damage parameters for all the cases considered.*

	D1.A		D2.A		D1.B		D2.B	
	$\lvert s_e^D - s^D \rvert$	$\lvert h_e^D - h^D \rvert$	$\lvert s_e^D - s^D \rvert$	$\lvert h_e^D - h^D \rvert$	$\lvert s_e^D - s^D \rvert$	$\lvert h_e^D - h^D \rvert$	$\lvert s_e^D - s^D \rvert$	$\lvert h_e^D - h^D \rvert$
H	0	0.028	0	0.087	0.024	0.014	0.004	0.031
Bartlett	0	0.409	0	0.226	0.062	0.194	0.023	0.063
MVDR	0	0.028	0	0.087	0.024	0.014	0.004	0.031

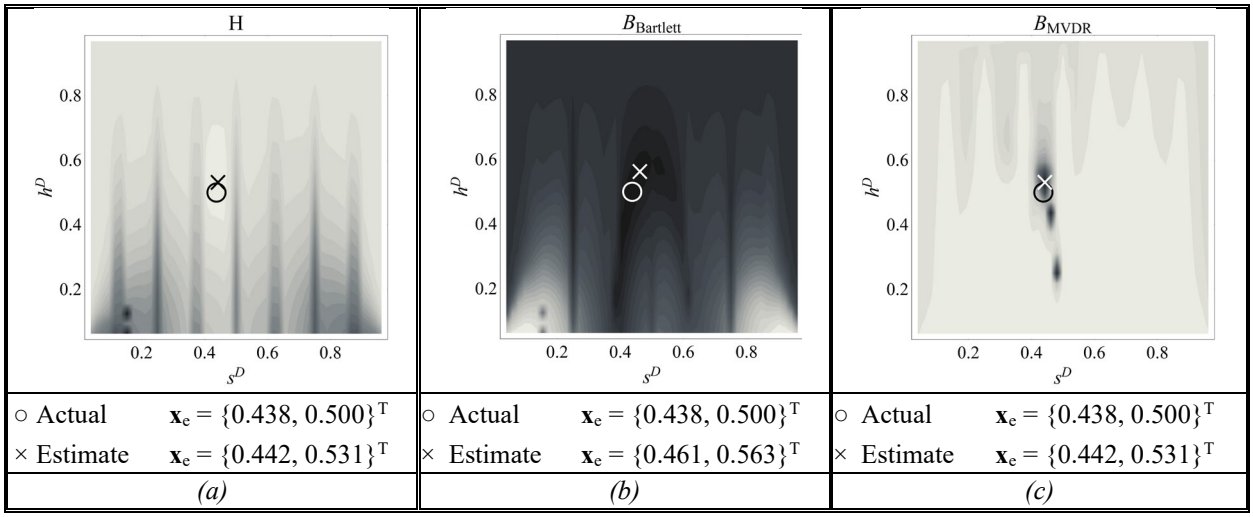

Figure 7. *Contour plots and estimates of the objective function a), Bartlett beamformer b) and MVDR c) for D2.B.*

Conclusions

We examined the possibility of applying to damage identification some beamforming algorithms which are widely used in fields such as underwater source identification and image processing. The identification of damage using experimental modal curvatures revealed that the use of MVDR is reliable and it suppresses local extrema which may lead to erroneous estimates. All the processors under investigation have exhibited high sensitivity to damage location, although MVDR appeared to be the most sensitive with regard to damage intensity.

References

[1] C. R. Farrar, S. W. Doebling, Damage detection II: field applications to large structures. In: J. M. M. Silva and N. M. M. Maia (eds.), Modal analysis and testing, Nato Science Series, Kluwer Academic Publishers, Dordrecht, Netherlands, 1999.

[2] A. Pandey, M. Biswas, M. Samman, Damage detection from changes in 465 curvature mode shapes, Journal of Sound and Vibration 145 (2) (1991) 321–332. https://doi.org/10.1016/0022-460X(91)90595-B

[3] M. Dilena, A. Morassi, M. Perin, Dynamic identification of a reinforced concrete damaged bridge, Mechanical Systems and Signal Processing 25 (8) (2011) 2990–3009. https://doi.org/10.1016/j.ymssp.2011.05.016

[4] G. Turek, W. Kuperman, Applications of matched-field processing to structural vibration problems, The Journal of the Acoustical Society of America 495 101 (3) (1997) 1430–1440. https://doi.org/10.1121/1.418168

[5] S. Sternini, A. Pau and F. Lanza di Scalea, "Minimum Variance Imaging in Plates Using Guided Wave Mode Beamforming," IEEE Transactions on Ultrasonics, Ferroelectrics and Frequency Control, 66 (12), 1906-1919 (2019). https://doi.org/10.1109/TUFFC.2019.2935139

[6] F. Vestroni, A. Pau, J. Ciambella, "The role of curvatures in damage identification" in IABMAS Proceedings, Barcelona, Spain, 11-15 July 2022, page 1-8, (2022).

[7] A. Pau, U. Eroglu, Identification of damage in beams using the Minimum Variance Distorsionless Response beamformer, submitted